On the rate and gravitational wave emission of short and long GRBs

Jorge Armando Rueda Hernández – ICRANet

(On behalf of a larger collaboration)

R. Ruffini[1,2,3,4], J. Rodriguez[1,2], M. Muccino[1,2], J. A. Rueda[1,2,4], Y. Aimuratov[1,2], U. Barres de Almeida[4,5], L. Becerra[1,2], C. L. Bianco[1,2], C. Cherubini[6,7], S. Filippi[6,7], D. Gizzi[1], M. Kovacevic[1,2,3], R. Moradi[1,2], F. G. Oliveira[1,2,3]. G. B. Pisani[1,2]. Y. Wang[1,2]

International Conference on Gravitation: Joint Conference of ICGAC-XIII and IK15

July 3-7, Seoul 2017

Gamma-ray bursts and neutron-star physics

Short GRBs:
NS-NS and NS-BH Mergers

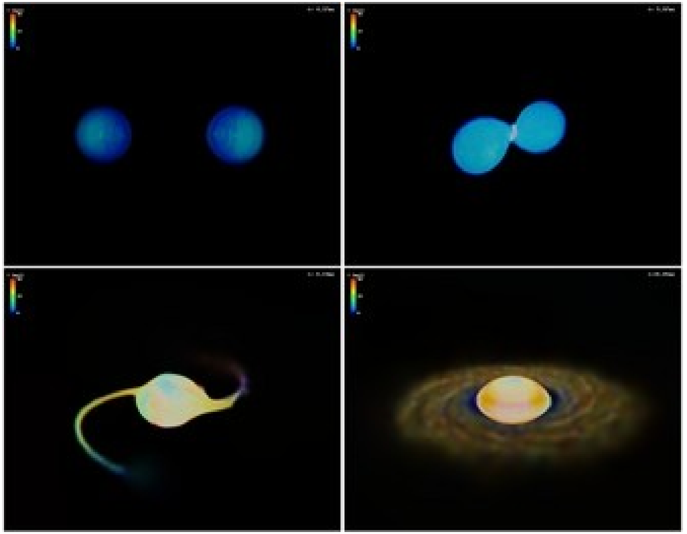

Long GRB-SN: Induced Gravitational Collapse

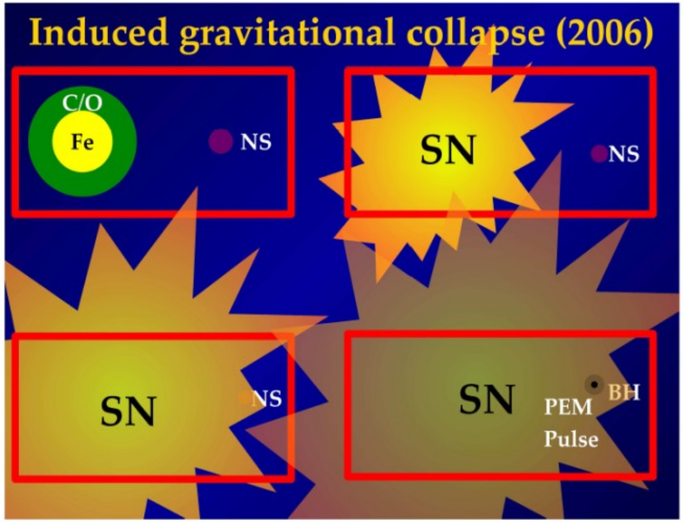

Long and short GRB subclasses

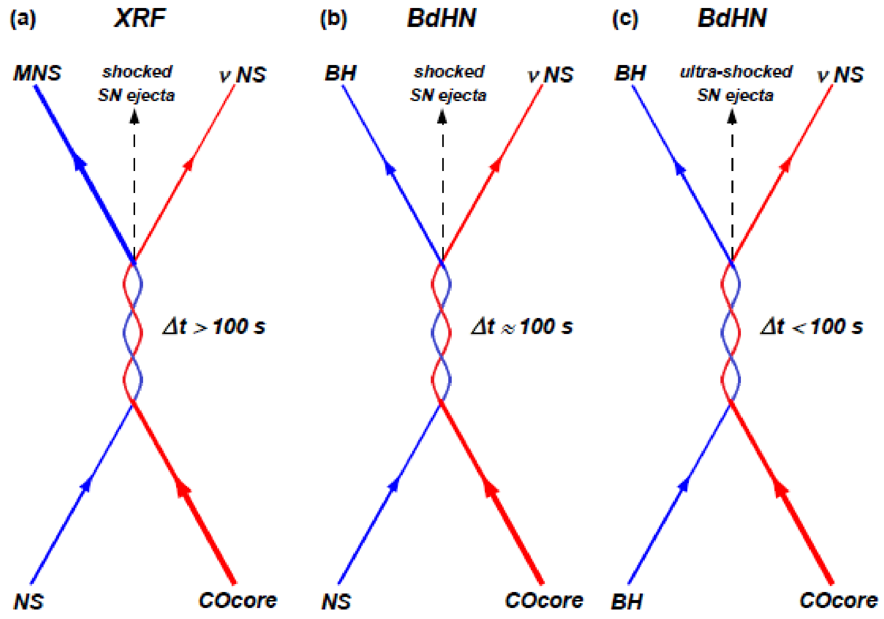

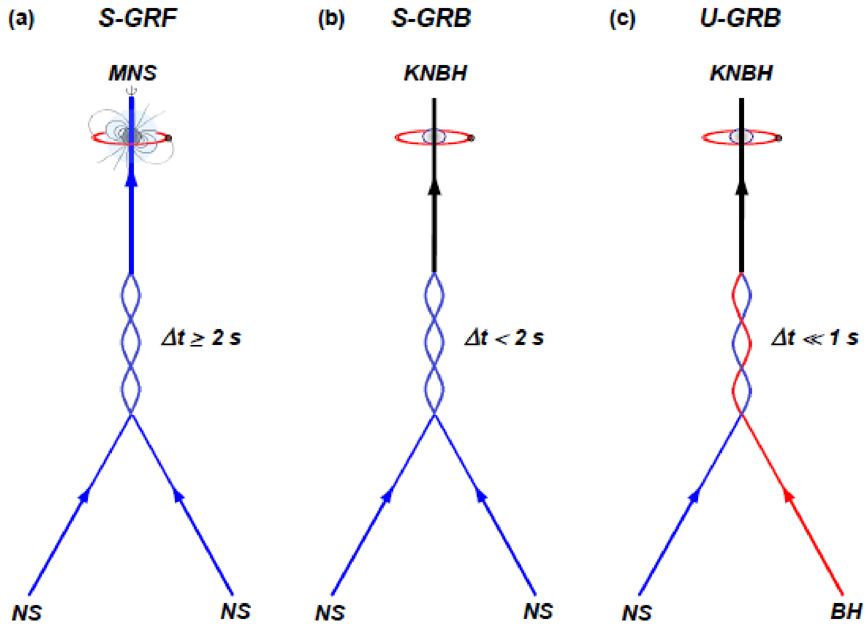

Ruffini et al., ApJ (2015,2016); R. Ruffini's talk (Monday 03/07/2017)

Short and long GRB sub-classes

Table 1. Summary of the astrophysical aspects of the different GRB sub-classes and of their observational properties. In the first four columns we indicate the GRB sub-classes and their corresponding *in-states* and the *out-states*. In columns 5–8 we list the ranges of $E_{p,i}$ and E_{iso} (rest-frame 1–10^4 keV), $E_{iso,X}$ (rest-frame 0.3–10 keV), and $E_{iso,GeV}$ (rest-frame 0.1–100 GeV). Columns 9 and 10 list, for each GRB sub-class, the maximum observed redshift and the local observed rate ρ_{GRB} obtained in Ruffini et al. (2016b).

	Sub-class	*In-state*	*Out-state*	$E_{p,i}$ (MeV)	E_{iso} (erg)	$E_{iso,X}$ (erg)	$E_{iso,Gev}$ (erg)	z_{max}	ρ_{GRB} ($Gpc^{-3}yr^{-1}$)
I	XRFs	CO_{core}-NS	νNS-NS	$\lesssim 0.2$	$\sim 10^{48}$–10^{52}	$\sim 10^{48}$–10^{51}	–	1.096	100^{+45}_{-34}
II	BdHNe	CO_{core}-NS	νNS-BH	~ 0.2–2	$\sim 10^{52}$–10^{54}	$\sim 10^{51}$–10^{52}	$\lesssim 10^{53}$	9.3	$0.77^{+0.09}_{-0.08}$
III	BH-SN	CO_{core}-BH	νNS-BH	$\gtrsim 2$	$> 10^{54}$	$\sim 10^{51}$–10^{52}	$\gtrsim 10^{53}$	9.3	$\lesssim 0.77^{+0.09}_{-0.08}$
IV	S-GRFs	NS-NS	MNS	$\lesssim 2$	$\sim 10^{49}$–10^{52}	$\sim 10^{49}$–10^{51}	–	2.609	$3.6^{+1.4}_{-1.0}$
V	S-GRBs	NS-NS	BH	$\gtrsim 2$	$\sim 10^{52}$–10^{53}	$\lesssim 10^{51}$	$\sim 10^{52}$–10^{53}	5.52	$(1.9^{+1.8}_{-1.1}) \times 10^{-3}$
VI	U-GRBs	νNS-BH	BH	$\gtrsim 2$	$> 10^{52}$	–	–	–	$\gtrsim 0.77^{+0.09}_{-0.08}$
VII	GRFs	NS-WD	MNS	~ 0.2–2	$\sim 10^{51}$–10^{52}	$\sim 10^{49}$–10^{50}	–	2.31	$1.02^{+0.71}_{-0.46}$

Ruffini et al., ApJ (2015,2016); arXiv: 1602.02732

Short GRBs

NS+NS → MNS

NS+NS → BH

Two sub-classes of short GRBs

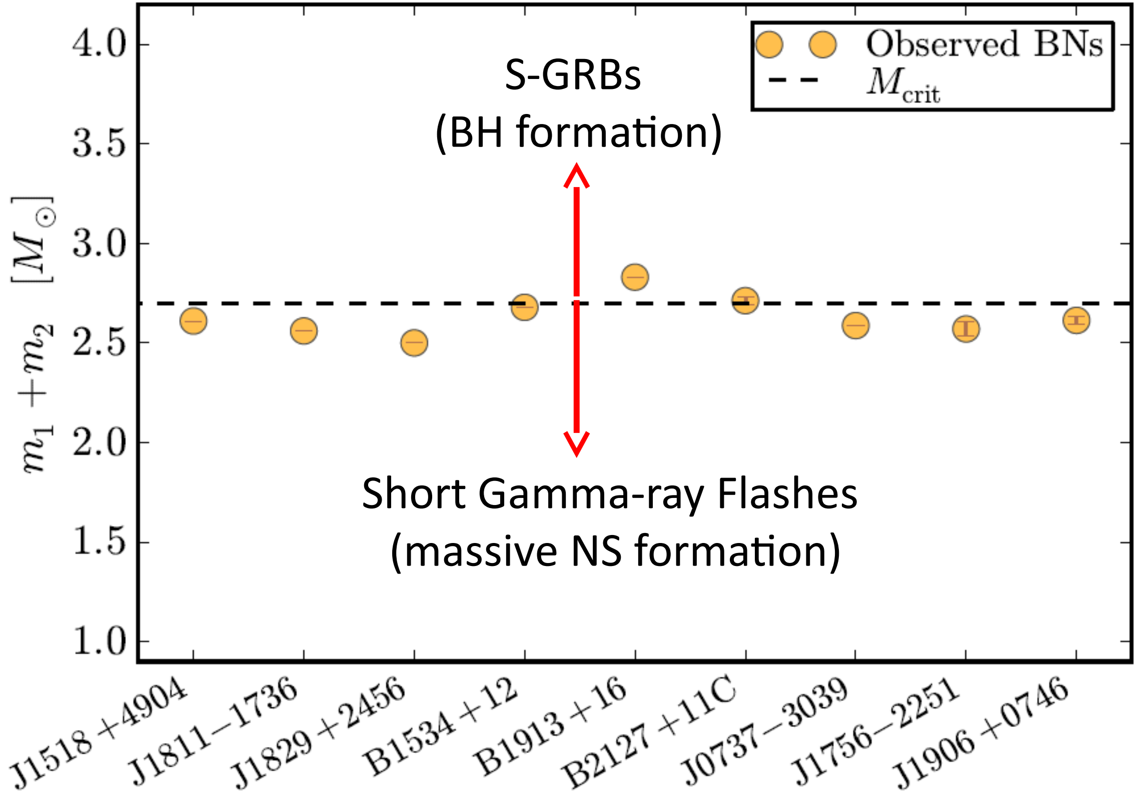

NS mass distribution in BNS peaks at 1.32 M_{sun}

(Kiziltan et al. 2013)

So:

M_{BNS} ~ 2.64 M_{sun}

(neglecting NS binding energy and angular momentum)

Ruffini et al., ApJ (2015); arXiv: 1412.1018v4

Neutron Star Binding Energy

(Cipolletta et al., PRD 2015; arXiv: 1506.05926; Cipolletta et al., PRD in press; arXiv:1612.02207)

Static Configurations

$$\frac{M_b}{M_\odot} \approx \frac{M}{M_\odot} + \frac{13}{200}\left(\frac{M}{M_\odot}\right)^2$$

Rotating Configurations

c J/(G M^2_{sun})

$$\frac{M_b}{M_\odot} = \frac{M}{M_\odot} + \frac{13}{200}\left(\frac{M}{M_\odot}\right)^2\left(1 - \frac{1}{130}j^{1.7}\right)$$

Which are the mass and angular momentum of the merged core: NS+NS → MNS?

Depends on:

1) Mass-ratio of the binary (M1/M2 ~1 for the galactc BNS)

2) Degree at which baryon mass is conserved

3) Degree at which angular momentum is conserved

$$(M_1, M_2) \rightarrow (M_{b1}, M_{b2})$$
$$M_{bf} = \alpha\,(M_{b1} + M_{b2}); \quad \alpha \sim 1$$

$$J_{mc} = \eta\, J_i \sim \eta\, J_{bin} \text{ (merger instant)}$$

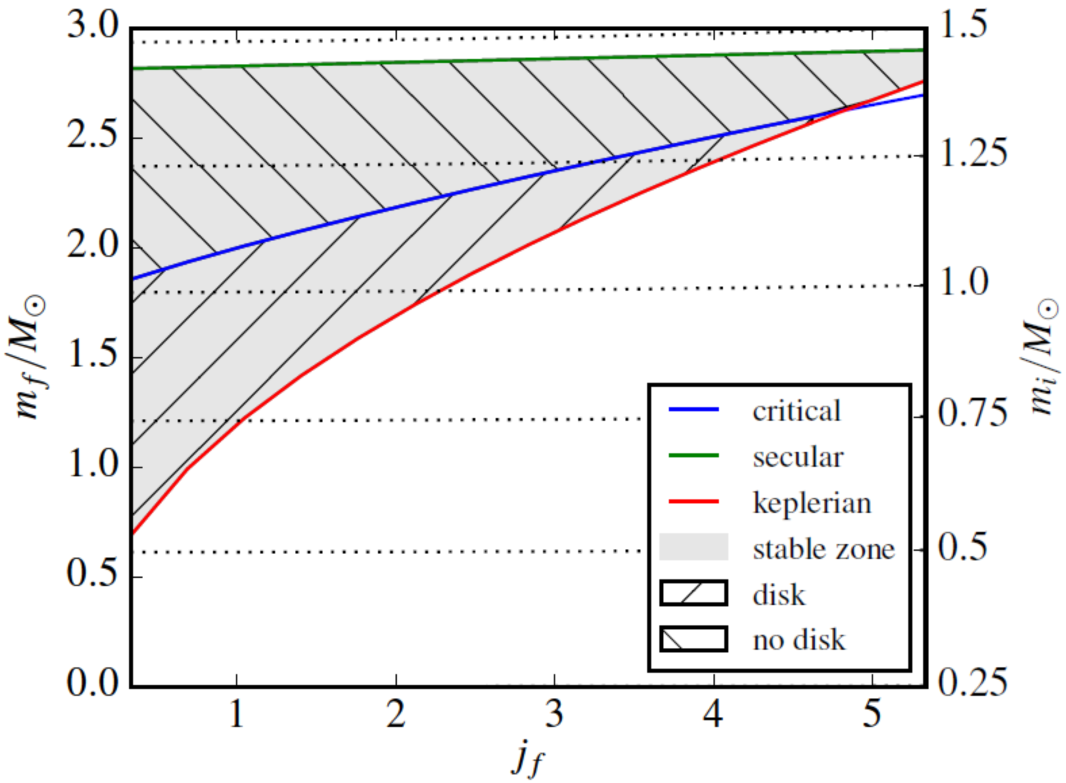

NS+NS→ BH ?

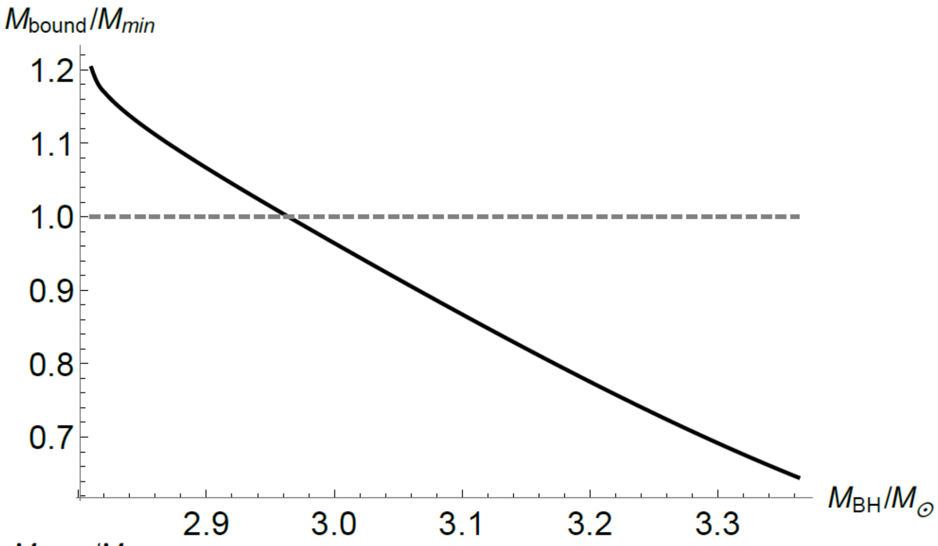

The explanation of the observed GeV emission in S-GRBs by accretion onto the formed BH may constraint the BH properties and the merging NS masses !

Aimuratov, Ruffini, et al.; ApJ in press; arXiv:1704.08179
Ruffini, Muccino, et al.; ApJ 2016; arXiv:1607.02400
Ruffini, Muccino, et al.; ApJ 2016; arXiv:1412.1018

See also M. Muccino's talk; Friday 06/07/2017

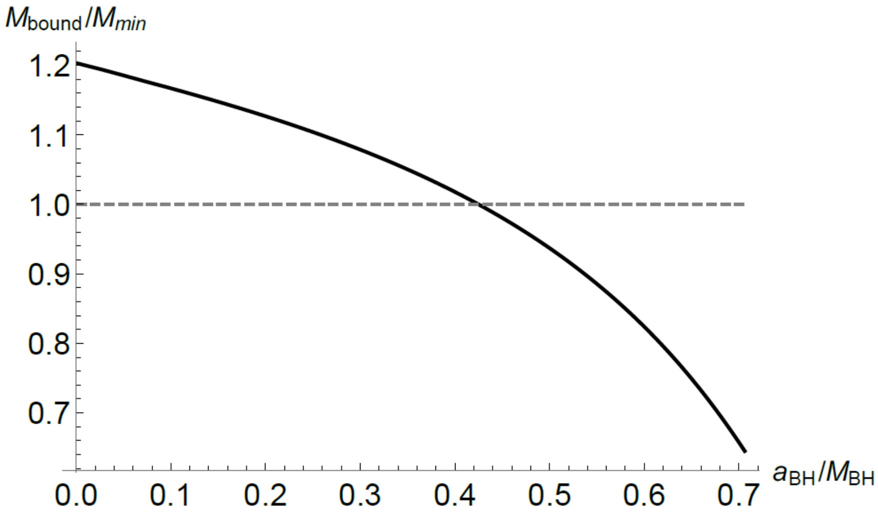

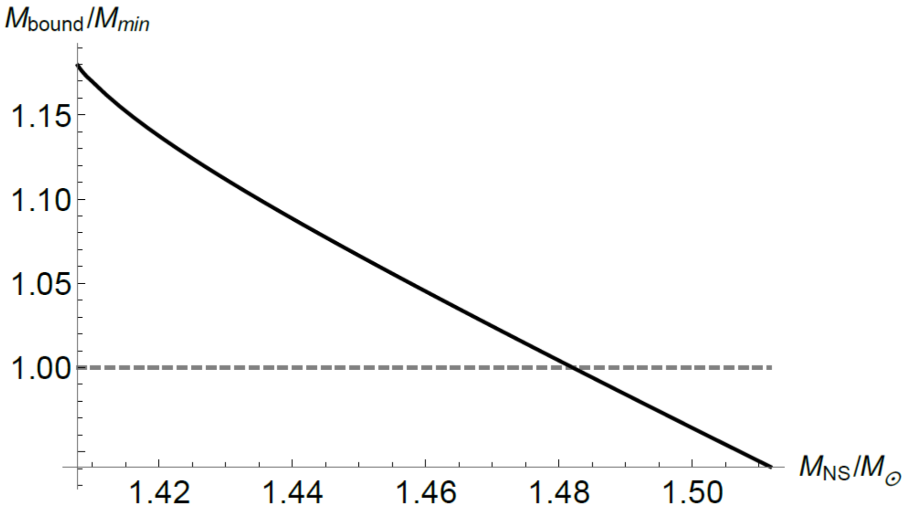

Long GRBs

CO+NS → NS+MNS

CO+NS → NS+BH

Binary-Driven Hypercritical Accretion

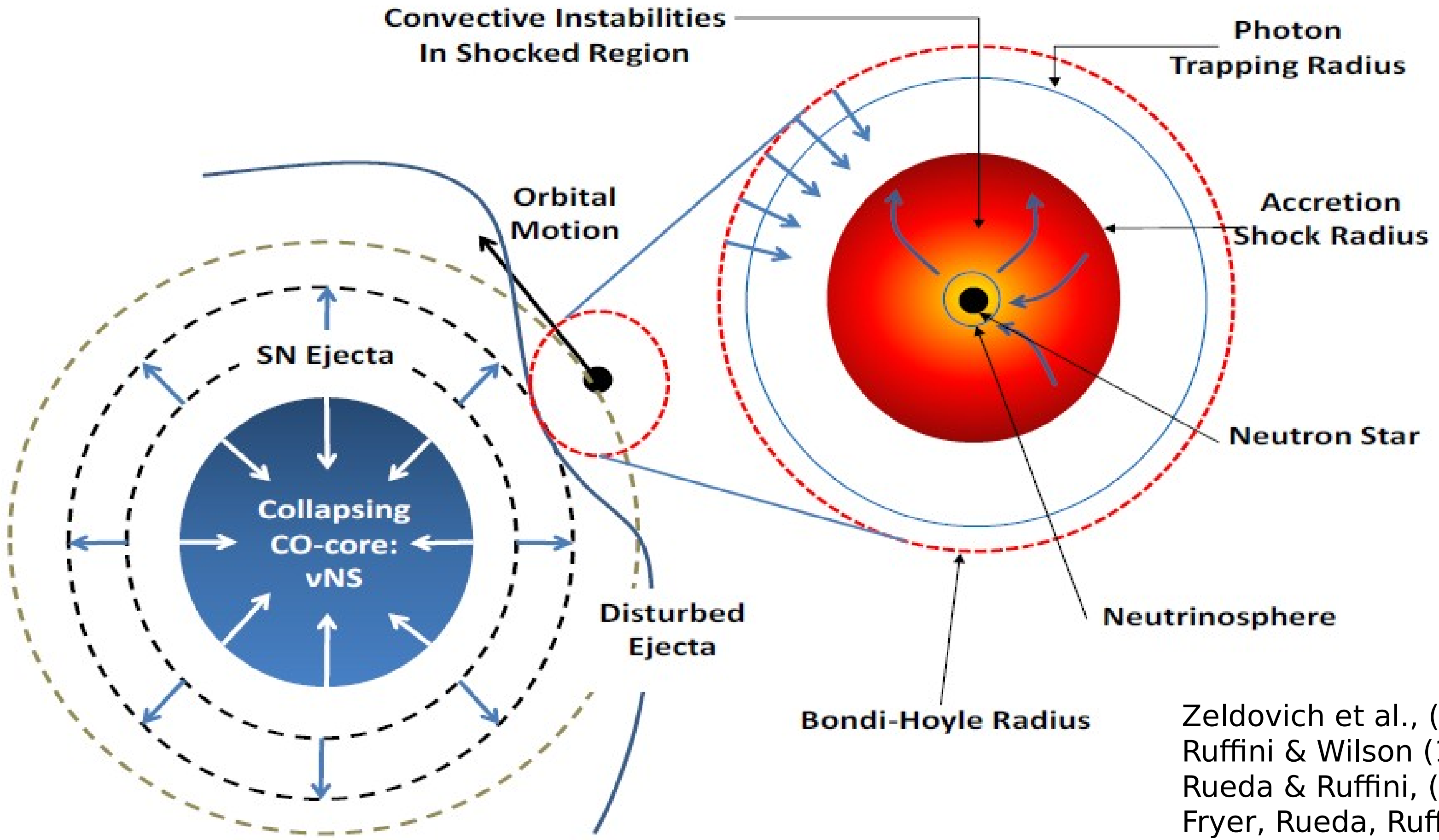

Zeldovich et al., (1972)
Ruffini & Wilson (1973)
Rueda & Ruffini, (2012)
Fryer, Rueda, Ruffini, ApJL (2014)

Supernova ejecta at t=0

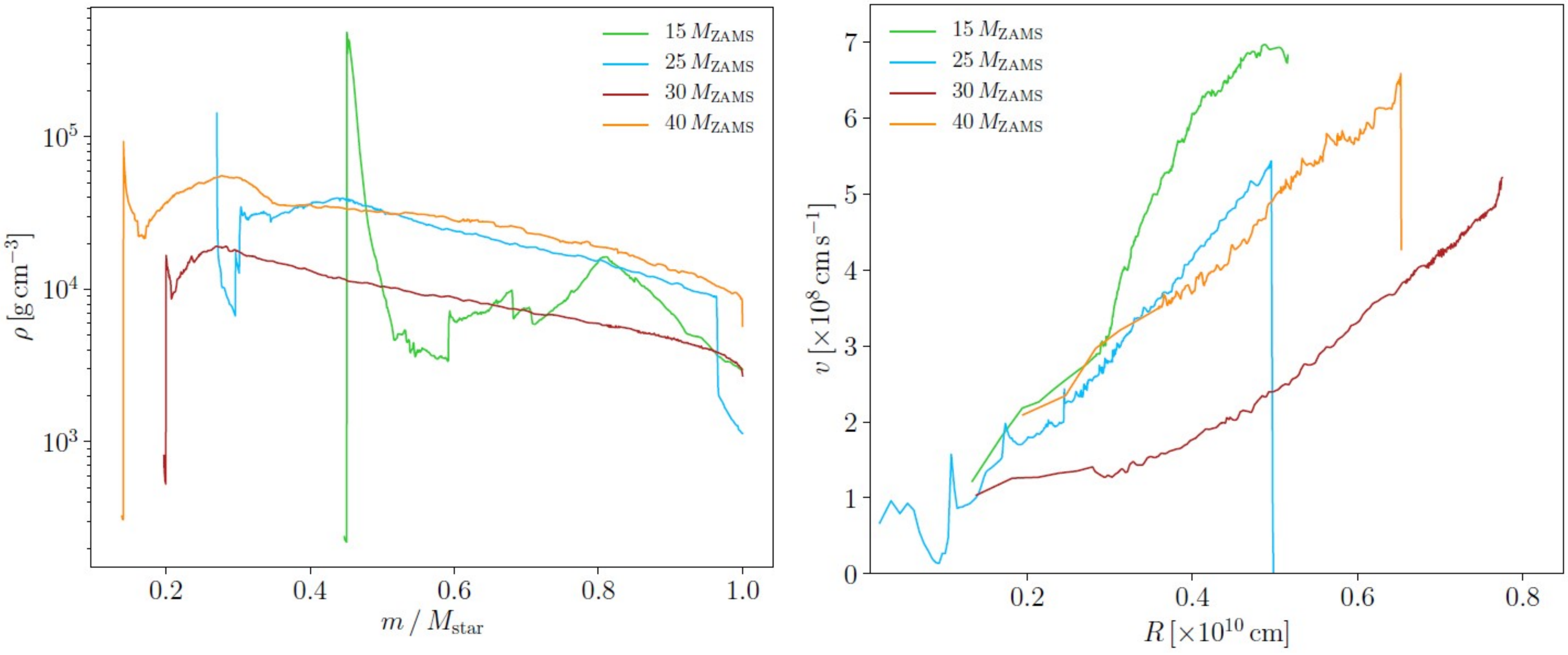

Becerra, et al., in preparation
L. Becerra's talk on Monday 03/07/2017

Visualizing the IGC process

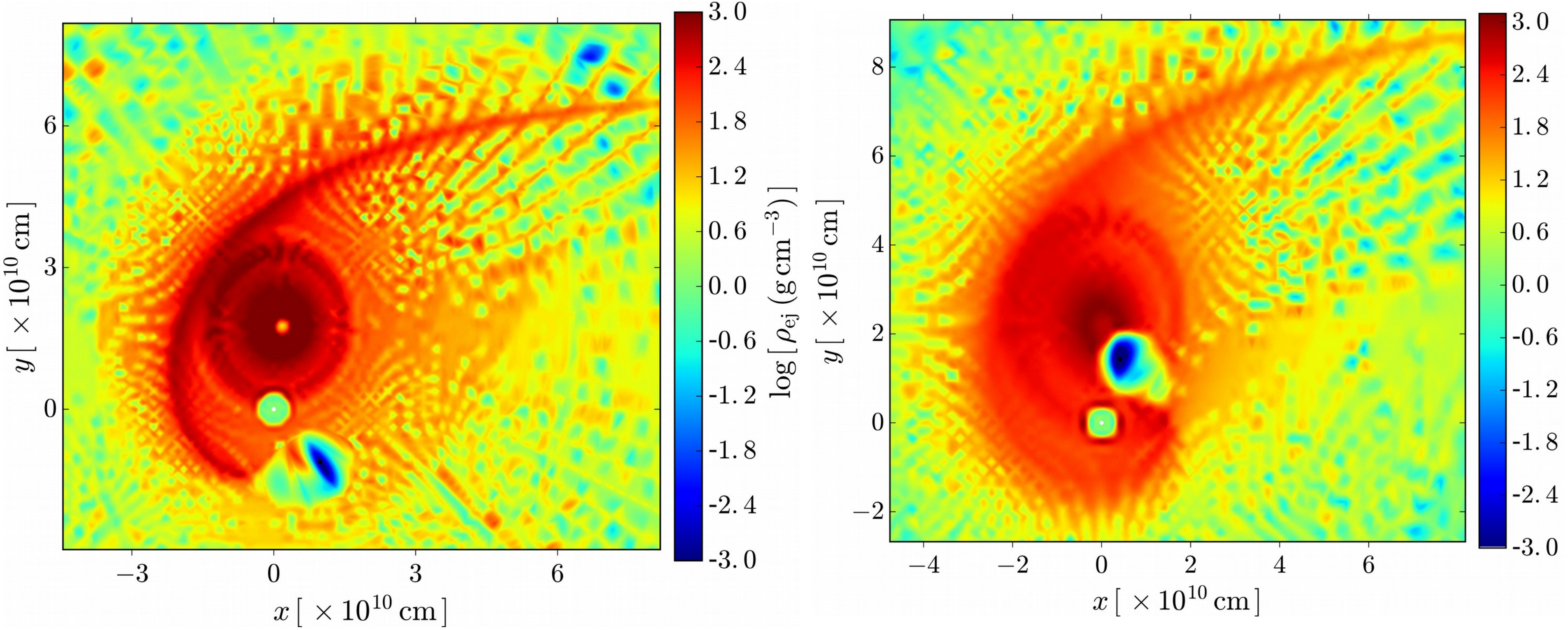

Becerra, Bianco, Fryer, Rueda, Ruffini, ApJ 2016;arXiv:1606.02523

L. Becerra's talk
Monday 03/07/2017

Latest ICRANet-LANL simulations

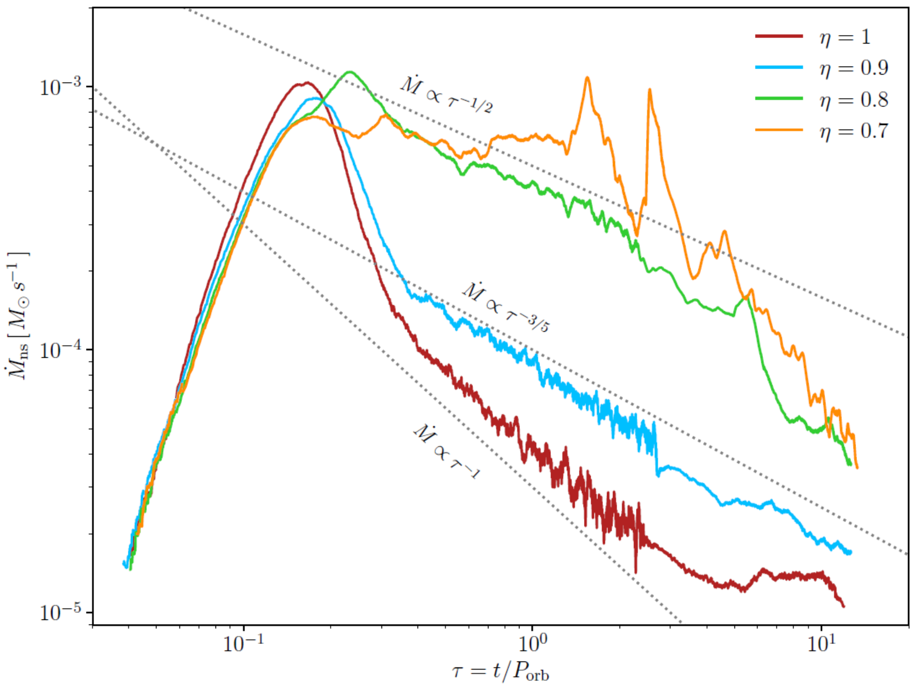

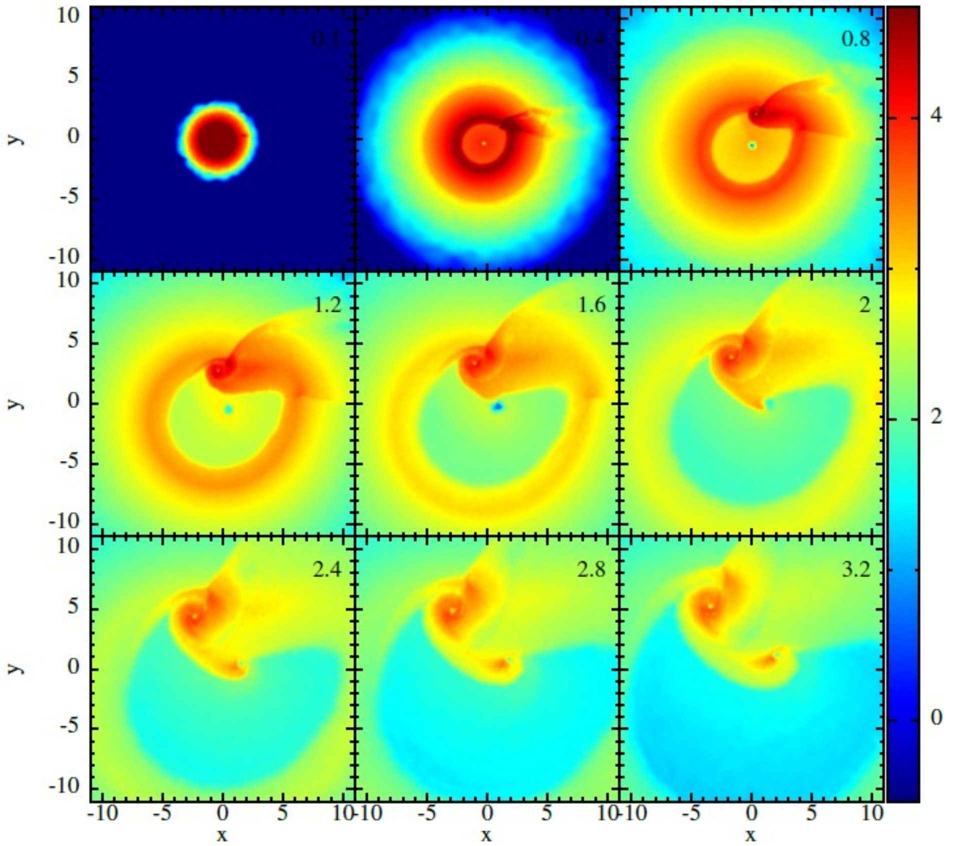

Becerra, et al., in preparation
L. Becerra's talk on Monday 03/07/2017

Latest ICRANet-LANL simulations

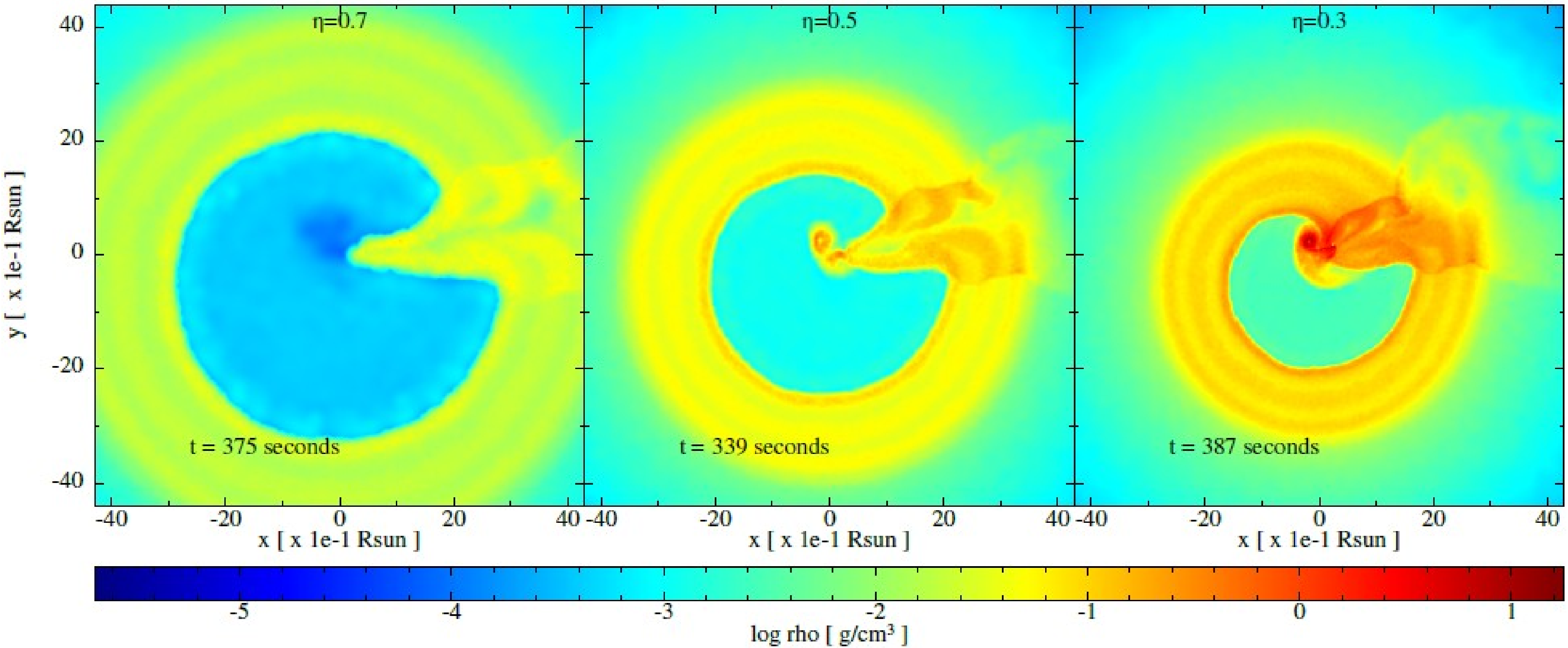

Becerra, et al., in preparation
L. Becerra's talk on Monday 03/07/2017

NS evolution up to the instability point

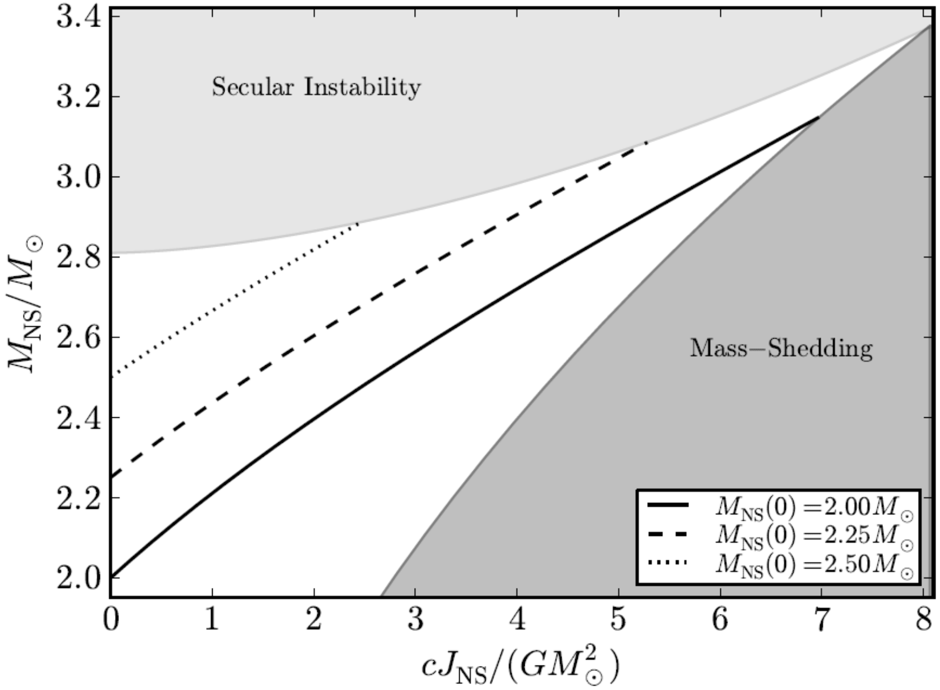

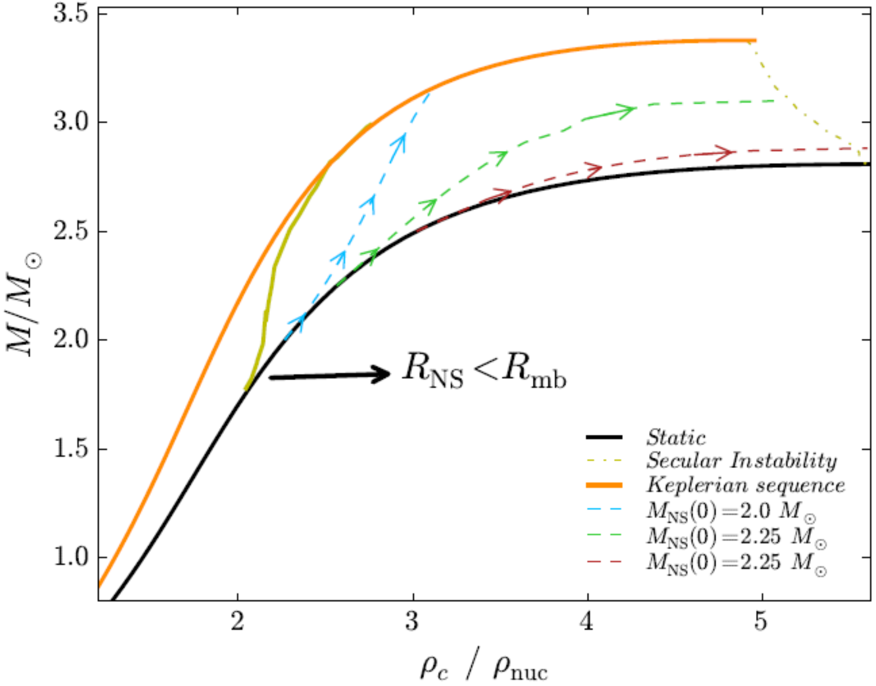

Becerra, Cipolletta, Fryer, Rueda, Ruffini, ApJ 2015; arXiv: 1505.07580

NS-BH binaries produced by BdHNe

(Fryer, Oliveira, Rueda, Ruffini, Phys. Rev. Lett 2015; arXiv:1505.02809)

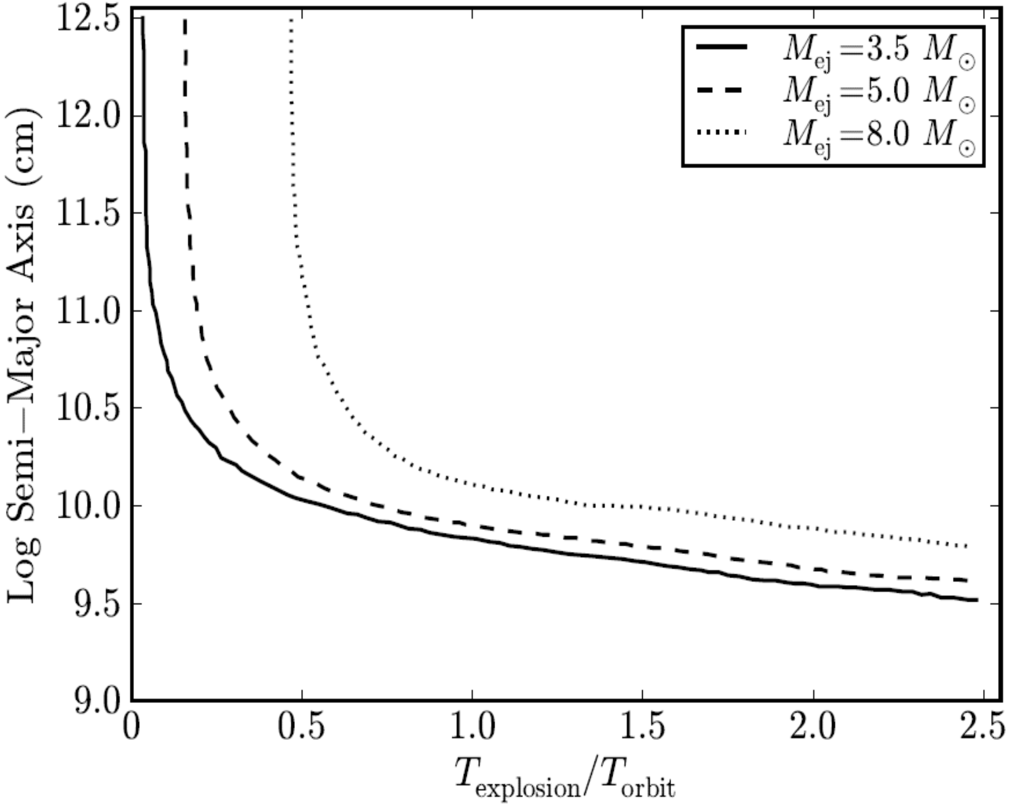

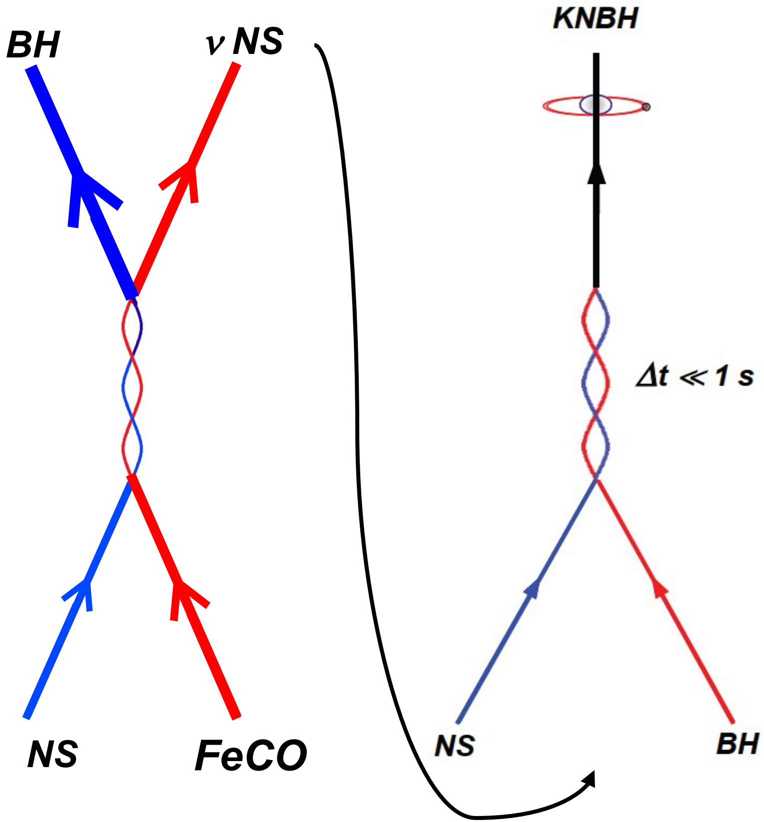

X-ray Flashes - BdHNe Separatrix

(Becerra, Bianco, Fryer, Rueda, Ruffini, ApJ 2016; arXiv:1606.02523)

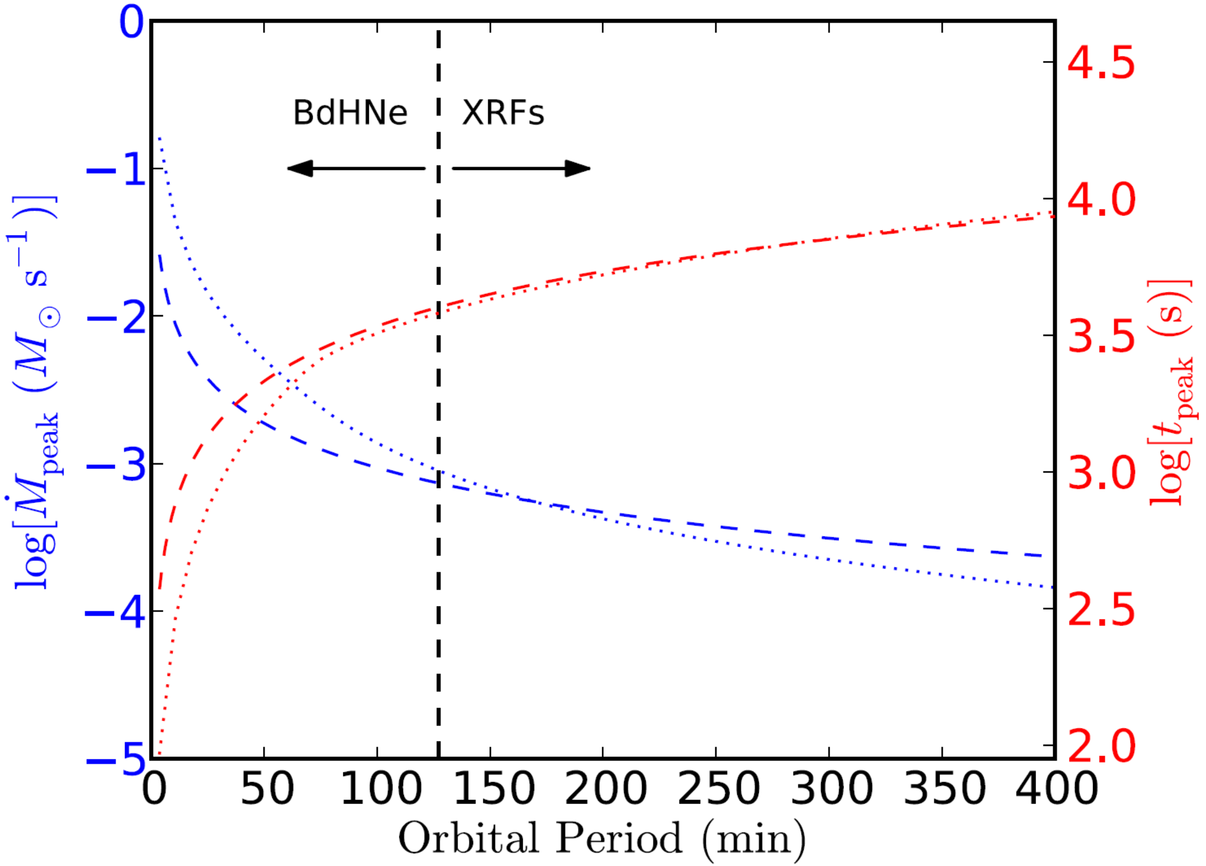

Short and long GRB subclasses

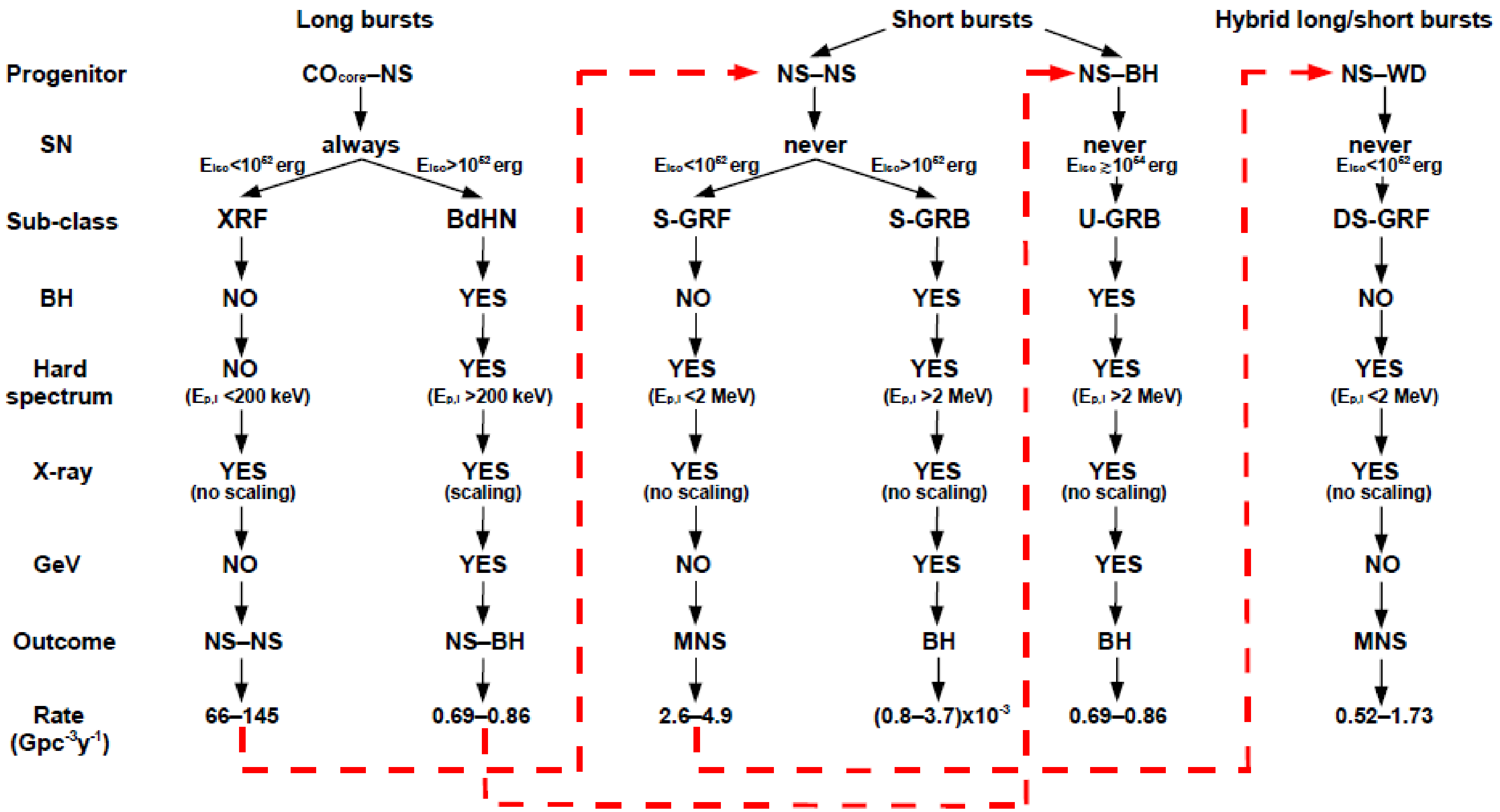

Ruffini et al., ApJ (2015,2016)

Gravitational-wave detectability of GRBs

$$\rho^2 = 4\int_0^\infty \frac{|\tilde{h}(f)|^2}{S_n(f)}df$$

$$\langle\rho^2\rangle = 4\int_0^\infty \frac{\langle|\tilde{h}(f)|^2\rangle}{S_n(f)}df = 4\int_0^\infty \frac{h_c^2(f)}{f^2 S_n(f)}df$$

$$h_c = \frac{(1+z)}{\pi d_l}\sqrt{\frac{\langle F_+^2\rangle}{2}\frac{G}{c^3}\frac{dE}{df_s}[(1+z)f]}$$

We can estimate the signal-to-noise ratio with the gravitational-wave spectrum

Strong-field GW emission in Schwarzschild and Kerr geometries: some general considerations

J. F. Rodriguez' talk
Monday 4/07

$$H = -P_t = -N^i P_i + N\sqrt{m^2 + \gamma^{ij} P_i P_j},$$

$$\frac{dr}{dt} = \frac{\partial H}{\partial P_r},$$

$$\frac{d\phi}{dt} = \frac{\partial H}{\partial P_\phi},$$

$$\frac{dP_r}{dt} = -\frac{\partial H}{\partial r},$$

$$\frac{dP_\phi}{dt} = -\frac{1}{\omega}\frac{dE}{dt}.$$

Computed via Sasaki-Nakamura Method

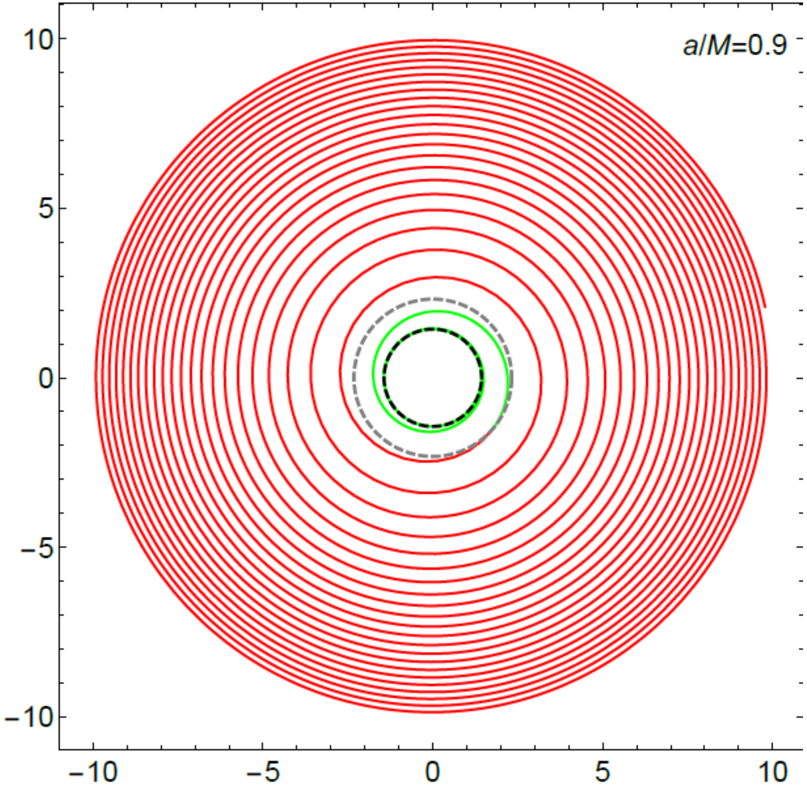

Rodriguez, Rueda, Ruffini, arXiv: 1706.06440

Strong-field GW emission in Schwarzschild and Kerr geometries: some general considerations

J. F. Rodriguez' talk
Monday 4/07

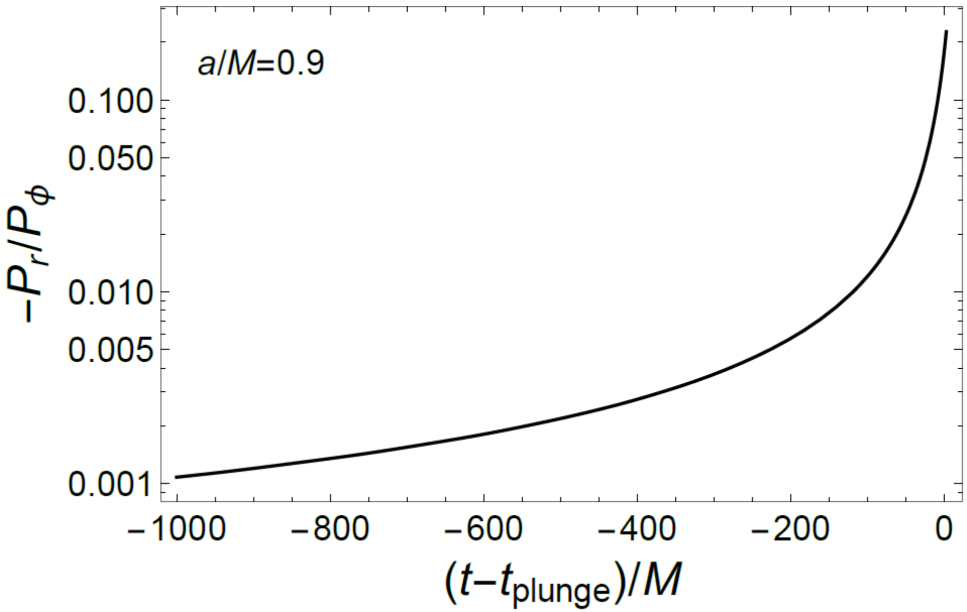

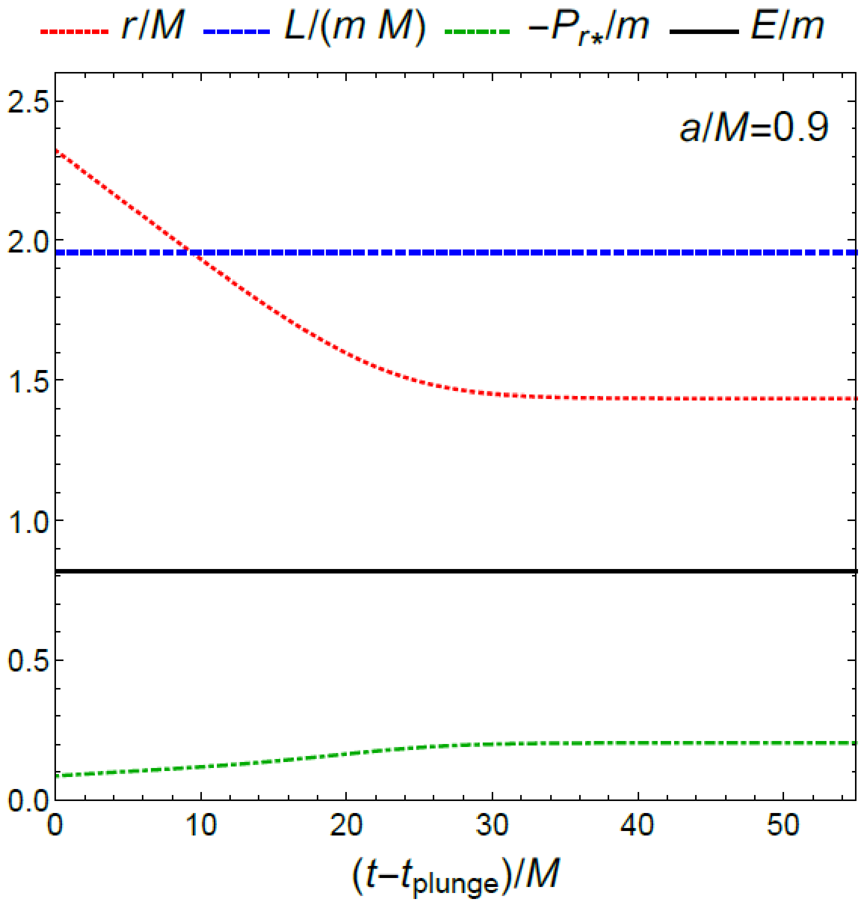

Rodriguez, Rueda, Ruffini, arXiv: 1706.06440

Test-particle helicoidal-drifting-sequence in the Kerr geometry vs. numerical-relativity waveform

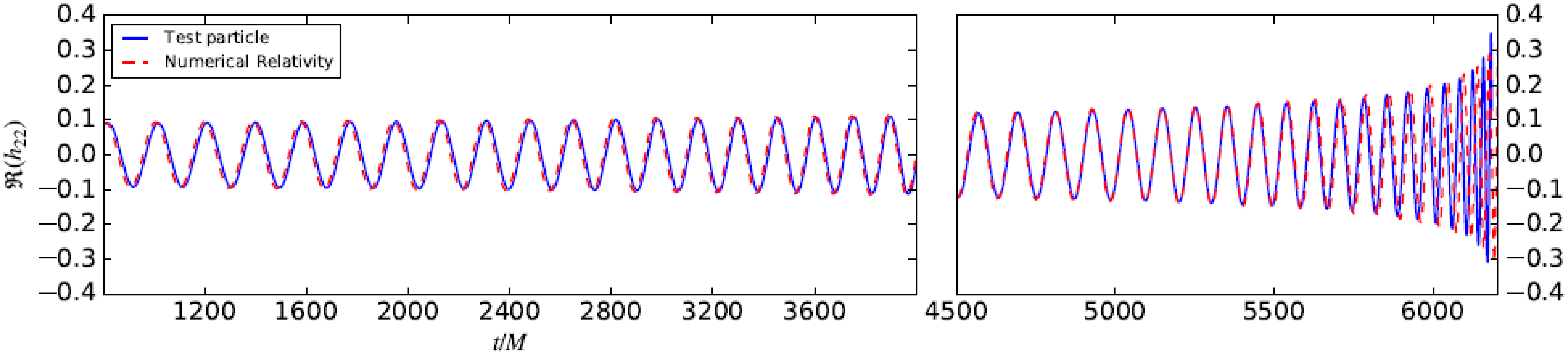

Rodriguez, Rueda, Ruffini, arXiv: 1706.07704
(last-week post)

J. F. Rodriguez' talk
Monday 4/07

Gravitational-wave spectrum during the helicoidal-drifting-sequence

$$\frac{dE}{df_s} = \frac{1}{3}(\pi G)^{2/3} M_c^{5/3} f_s^{-1/3}$$

$$f_s = 2 f_{\rm orb}$$

$$M_c = \mu^{3/5} M^{2/5} = \nu^{3/5} M$$

~ power-law spectrum up to near the last circular orbit (LCO) or up to the "contact" distance in the case of NS-NS mergers

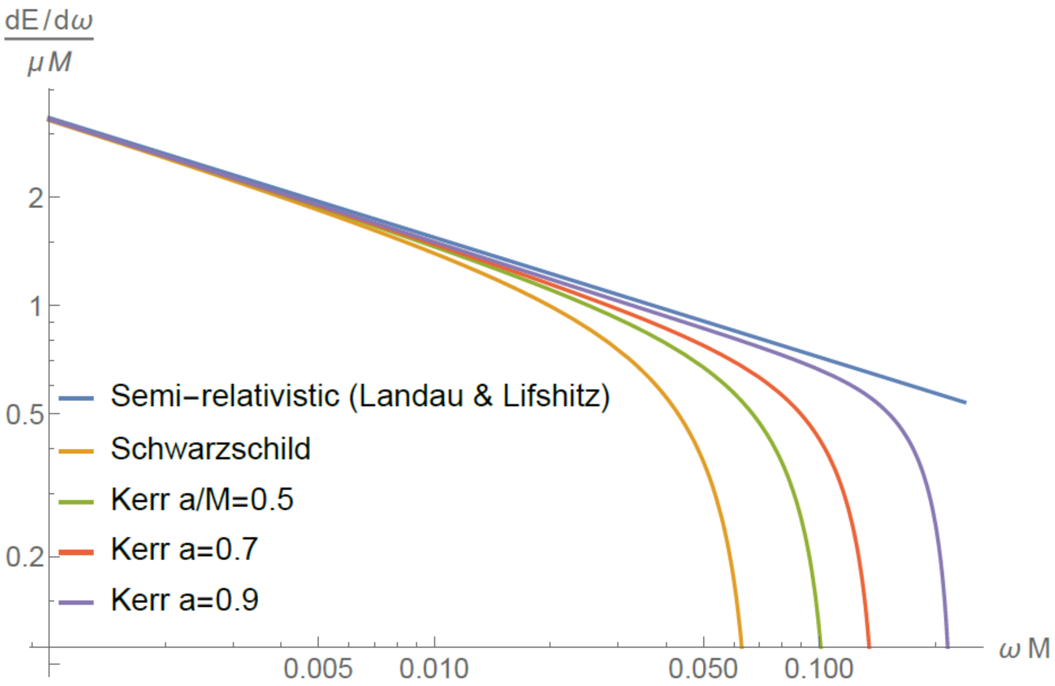

GW spectrum during the final smooth merger?

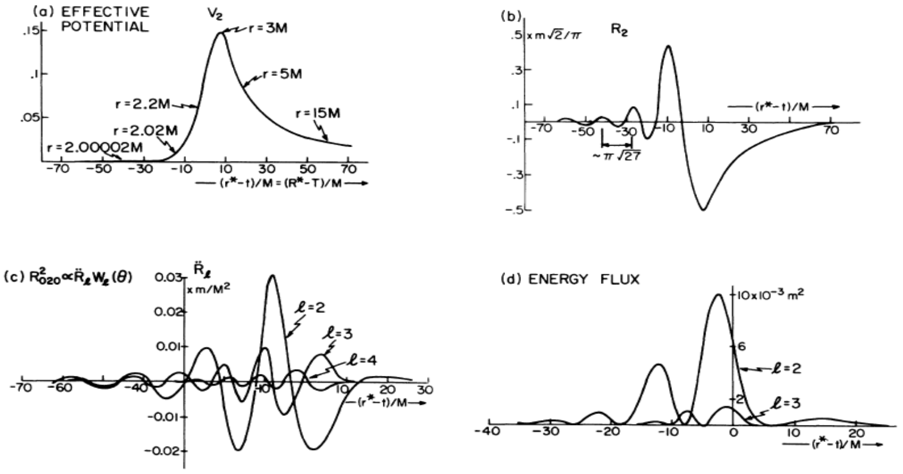

FIG. 1. Asymptotic behavior of the outgoing burst of gravitational radiation compared with the effective potential, as a function of the retarded time $(t-r^*)/M$. (a) Effective potential for $l=2$ in units of M^2 as a function of the retarded time $(t-r^*)/M=(T-R^*)/M$. For selected points the value of the Schwarzschild coordinate r is also given. (b) Radial dependence of the outgoing field $R_l(r,t)$ as a function of the retarded time for $l=2$. (c) $\ddot{R}_l(r^*,t)$ factors of the Riemann tensor components (see text) given as a function of the retarded time for $l=2,3,4$. (d) Energy flux integrated over angles for $l=2,3$; the contributions of higher l are negligible.

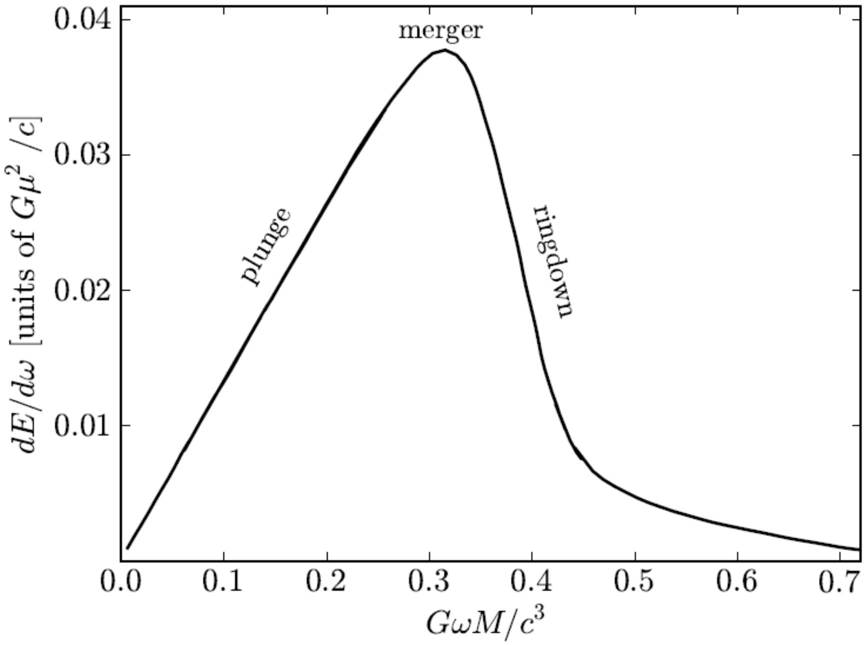

Davis, Ruffini, Press, Price, Phys. Rev. Lett. 27, 1466 (1971)
Davis, Ruffini, Tiomno, Phys. Rev. D 5, 2932 (1972)

Helicoidal-drifting-sequence (HDS)

$$\frac{dE}{df_s} = \frac{1}{3}(\pi G)^{2/3} M_c^{5/3} f_s^{-1/3}$$

Approximately up to very close the last circular orbit (LCO) or up to the “contact”

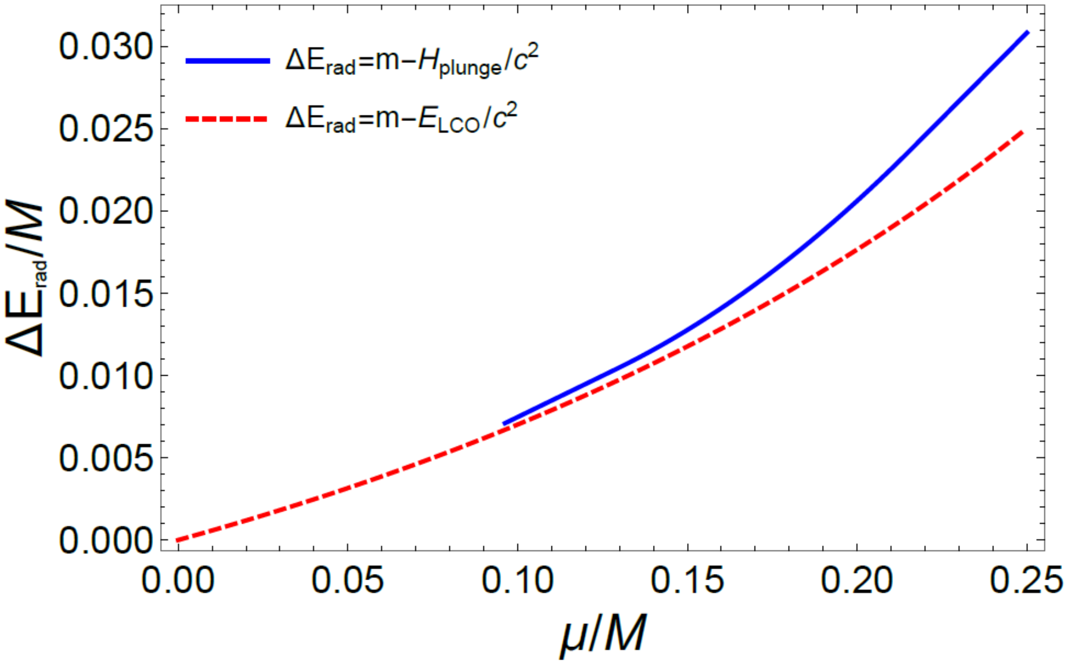

NS+NS

$$f_{\rm merger}^{\rm NS-NS} \approx f_{\rm contact}^{\rm NS-NS} = \frac{1}{\pi}\frac{c^3}{GM}\left[\frac{\mathcal{C}_1\mathcal{C}_2(1+q)}{\mathcal{C}_1 + q\mathcal{C}_2}\right]^{3/2}$$

NS+BH

$$f_{\rm plunge}^{\rm NS-BH} \approx \frac{1}{\pi}\left(\frac{GM}{r_{\rm LSO}^3}\right)^{1/2} = \frac{1}{\pi 6^{3/2}}\left(\frac{c^3}{GM}\right)$$

Rodriguez, Rueda, Ruffini, arXiv: 1706.07704 (last-week post)

Ruffini, Rodriguez, Muccino, Rueda et al., arXiv: 1602.03545

Some properties of the relevant NS-NS and NS-BH mergers

	$\Delta E_{\rm insp}$ (erg)	$f_{\rm merger}$ (kHz)	$z_{\rm min}^{\rm obs}$	$d_{l_{\rm min}}$ (Mpc)	$d_{\rm GW}$ (Mpc) O1	$d_{\rm GW}$ (Mpc) 2022+
S-GRF	7.17×10^{52}	1.20	0.111	508.70	168.43	475.67
S-GRB	1.02×10^{53}	1.43	0.903	5841.80	226.62	640.18
U-GRB	1.02×10^{53}	0.98	0.169	804.57	235.62	665.72

Ruffini, Rodriguez, Muccino, Rueda et al., arXiv: 1602.03545

GW detectability by aLIGO, eLISA and resonant bars

Inspiral/merger

Solid/dots:
S-GRF: 1.4+1.4
Z=0.11, d=

Short-dashed/star :
S-GRB: 2.0+2.0
z=0.9

Dotted/triangle:
U-GRB: 1.5+3.0
z=0.17

Long-dashed/diamond:
U-GRB: 1.5+10
z=0.17

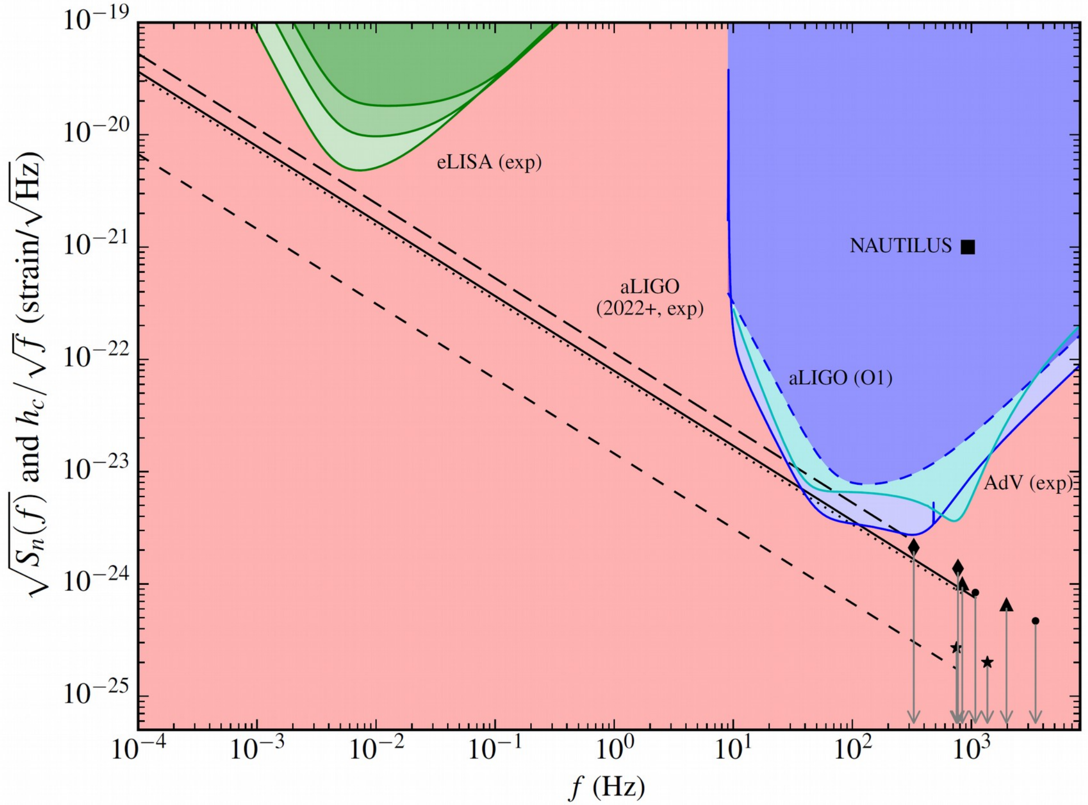

Ruffini, Rodriguez, Muccino, Rueda et al., arXiv: 1602.03545
aLIGO sensitivity from Abbott et al., Liv. Rev. Rel. 19 (2016)
ELISA sensitivity from Klein et al. PRD 93, 024003 (2016)
NAUTILUS sensitivity from Astone et al., CQG 25, 114048 (2008)

Detectability of GRB GWs by aLIGO

Ruffini, Rodriguez, Muccino, Rueda et al., arXiv: 1602.03545

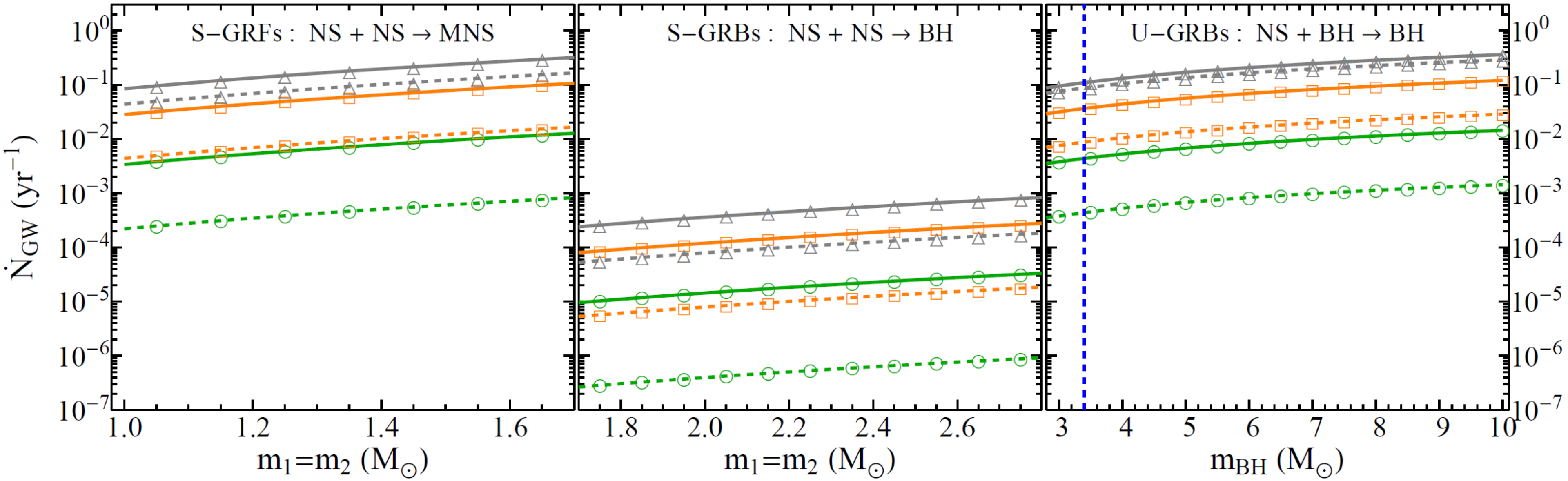

$$\dot{N}_{GW} = \rho_{GRB} V_{max}^{GW} \qquad V_{max}^{GW} = (4\pi/3)\mathcal{R}^3$$

R is the GW "range"; the values for aLIGO from: Abbott et al., Liv. Rev. Rel. 19 (2016)

IN CONCLUSION:

GRB sub-class	$\dot{N}_{\rm GRB}$ (yr^{-1})	$\dot{N}_{\rm GRB}^{\rm obs}$ (yr^{-1})	$\dot{N}_{\rm GW}$ (yr^{-1})
XRFs	144–733	1 (1997–2014)	undetectable
BdHNe	662–1120	14 (1997–2014)	undetectable
BH-SN	$\lesssim$ 662–1120	$\lesssim$ 14 (1997–2014)	undetectable
S-GRFs	58–248	3 (2005–2014)	O1: $(0.4–8)\times10^{-3}$ O3: 0.011–0.065 2022+: 0.1–0.2
S-GRBs	2–8	1 (2006–2014)	O1: $(0.4–8)\times10^{-6}$ O3: $(0.08–1.2)\times10^{-4}$ 2022+: $(0.8–3.6)\times10^{-4}$
U-GRBs	662–1120	–	O1: $(0.36–3.6)\times10^{-3}$ O3: 0.008–0.032 2022+: 0.076–0.095

For more details see: Ruffini, Rodriguez, Muccino, Rueda et al.; arXiv: 1602.03545